THE APPLICATION OF WINGLETS TO ROTORS

Th. van Holten
Delft University of Technology
Department of Aerospace Engineering
Delft, The Netherlands

Summary

The paper describes the preliminary results of theoretical and experimental research on winglets mounted on the blade tips of rotors. These winglets have the same effect as a duct around the propeller. The advantage might be a considerable saving in weight and structural complexity. The profile drag of the winglets requires careful optimization.

1. Introduction

As is well-known the efficiency of helicopter rotors and aircraft propellers is influenced beneficially, especially near the static conditions, by increasing the mass flow through the rotor plane. The most common way to achieve this is to increase the diameter. However, under certain circumstances the diameter of the rotor may be limited by the lay-out of the aircraft to a smaller value then would be desirable from a point of view of power considerations. Under such circumstances ducted configurations may be used, having the same mass increasing effect without the dimensional demands posed by large propellers. Although such ducts have serious disadvantages from the structural and weight point of view and penalize the cruising flight by additional drag, they are nevertheless used in special applications such as V/STOL aircraft, small hovering observation platforms, hovercraft and harbour tugboats.

An alternative to the duct system might be the rotor winglet system, which in principle could have the advantages of a duct whereas the structural demands are less.
Rotor winglets, or socalled tipvanes, should be shaped such that their leading edge is nearly perpendicular to the relative airflow at the blade tip, and that their lift acts in the direction of the rotor centre.
By reaction the tipvanes deflect the oncoming airflow radially outwards, thus decreasing the slipstream contraction and causing a mass-flow augmentation through the rotor. The system is aerodynamically fully comparable with a diffusing propeller duct, but a much smaller amount of structural material is needed and less components are required.

It is possible to derive a relatively simple theory predicting the potential performance improvements due to tipvanes. This theory, to be outlined in the paper, takes into account the drag losses associated with the tipvanes. Some time ago it was concluded from these theoretical considerations that the tipvane system might be very interesting, especially for the purpose of reducing the cost of windenergy. An experimental and theoretical research program was therefore initiated by Delft University of Technology in order to assess the practical feasibility of the system. Results obtained so far will be reported in the paper.
Although the mentioned research program was especially aimed at the application to windenergy systems, the results may be of interest for aeronautical applications as well. In a separate chapter the prospects for aeronautical applications will be considered.

2. Potential efficiency improvement by ducts or tipvanes.

As will be shown, the winglet or tipvane system induces a mean flow which is identical with that of a conventional duct system. Therefore, it may be well to recall a few classical relations between the thrust and power of ducted propellers, to show the potential improvements that are possible.

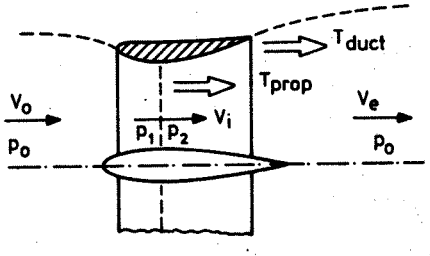

Fig. 1. Notations duct flow.

Fig. 1 shows the notations used. The forces shown are the forces exerted by the rotor or duct on the air. The thrust force of the duct finds its origin in the nose suction, well known from normal aerofoils. From momentum considerations it appears:

$$T_{prop} + T_{duct} = \rho V_1 \pi R^2 (V_e - V_o) \qquad (1)$$

By application of Bernoulli's law in turn between the stations 0→1 and 1→2, one finds the following expression for the force T_{prop}:

$$T_{prop} = \tfrac{1}{2}\rho\pi R^2 (V_e^2 - V_o^2) \qquad (2)$$

In the case of the free, unducted propeller, i.e.

for $T_{duct} = 0$, combination of eqs. (1) and (2) shows:

$$V_1 = \tfrac{1}{2}(V_o + V_e) \qquad (T_{duct} = 0) \tag{3}$$

which is the usual actuator disc result.

The presence of a duct (one of the diffusing, mass flow augmenting type) causes by induction the velocity V_1 in the rotorplane to be greater than usual, or: $V_1 > \tfrac{1}{2}(V_o + V_e)$. Let us write V_1 as:

$$V_1 = \tfrac{1}{2}(V_o + V_e) + \delta V \tag{4}$$

It follows from eqs. (1) and (2) that the propulsive force contributed by the duct is positive, and has the value:

$$T_{duct} = \rho\pi R^2\, \delta V\, (V_e - V_o) \tag{5}$$

Finally, by application of the energy-law it follows that the power ideally needed to generate the total thrust of the propeller-duct combination is given by:

$$P = \tfrac{1}{2}\rho V_1\, \pi R^2\, (V_e^2 - V_o^2) =$$

$$= \tfrac{1}{2}(V_o + V_e)\,.\,(T_{prop} + T_{duct}) \tag{6}$$

Conclusion: the formal relation between the total thrust and the power ideally needed is always the same, irrespective of whether a free propeller is considered or a ducted propeller. There are two differences between the two systems, however. The first is, that the ductsystem needs less diameter for the same performance, since the relatively thin duct carries a thrust force which would otherwise have to be generated by propellerblade extensions. Another difference is, that for a given total thrust the actual value of V_e is smaller in the case of a duct (see eq. (5)), so that quantitativelyrelation (6) between P and T is more favourable. The latter can of course be translated again in terms of improved diameter.

The question remaining is of course, how much the gain in diameter actually is. From the above given formulae one can derive the ratio R_{free}/R_{duct} expressing the diameter ratio between a free propeller and a ducted one for equal performance i.e. given thrust and given power.

In order to simplify the analysis and thereby to give a clear insight into the orders of magnitude involved, we will restrict the following to the static conditions (zero forward speed, or hovering flight).
In that case:

$$R_{free}/R_{duct} = \sqrt{1 + 2.\frac{\delta V}{V_e}} \tag{7}$$

or

$R_{free}/R_{duct} \approx \delta V/V_e$ for small δV.

According to an approximate analysis to be outlined later, one can estimate the velocity increment δV due to the duct as follows:

$$\frac{\delta V}{V_e} = \frac{\alpha/4}{\dfrac{2}{C_\ell . c/R} - \beta} \tag{8}$$

where C_ℓ = sectional liftcoefficient of the duct
c = duct chord.
α and β are functions of the duct geometry, given later in chapter 6 (eqs. (15) and (16)).

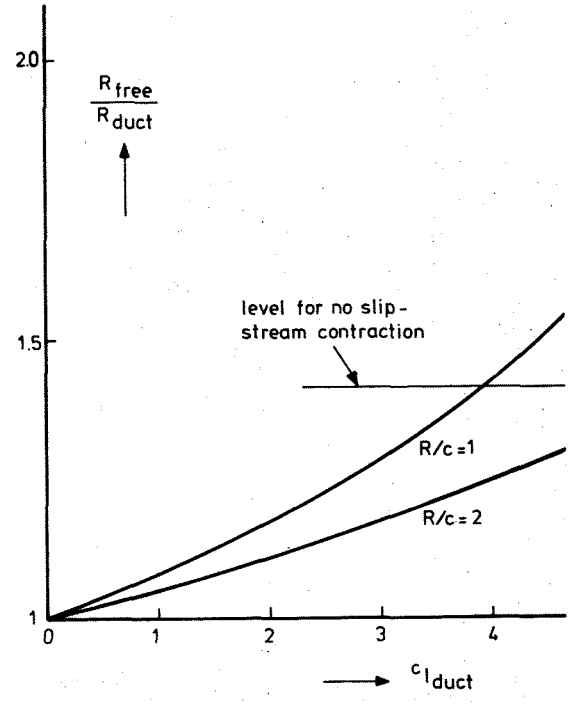

Fig. 2. Diameter ratio free and ducted propeller under static conditions. Given thrust and power.

Some results according to these very approximate formulae are shown in fig. 2. The results can also be expressed in a power ratio P_{free}/P_{duct} when both the thrust and diameter are given quantities:

$$\frac{P_{duct}}{P_{free}} = \frac{1}{\sqrt{1 + 2.\delta V/Ve}} \tag{9}$$

This relation is shown in fig. 3. Once again, these figures yield only an order of magnitude impression, and do not take into account any frictional losses.

The same order of improvement can in principle be achieved by application of winglets at the blade tips (tipvanes). They have, as will be shown, a mass-increasing effect similar to ducts, although at the cost of much less structural material and complexity. Research on tipvanes is being done at the Delft University of Technology with the particular application to windenergy in mind. Therefore, some remarks on the latter kind of application will be made first.

3. Some remarks on windturbines and concentrator systems.

The basic formula which forms the foundation of

all performance estimates of windmills, is an expression due to Betz:

$$P_{Betz} = \frac{16}{27} \tfrac{1}{2} \rho U^3 \pi R^2 \qquad (10)$$

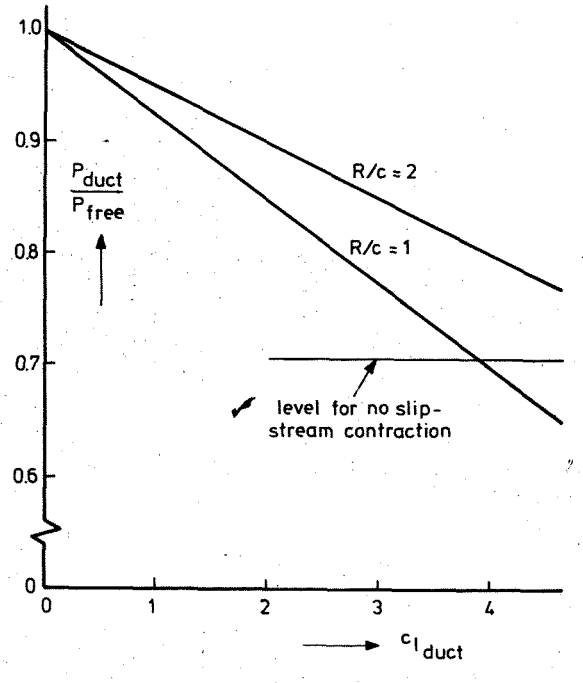

Fig. 3. Ideal power-ratio free and ducted propeller, under static conditions. Given thrust and diameter.

The expression states that the power output is ideally 16/27 of the kinetic energy flowing through a streamtube having the same diameter as the turbine-disc.
The power P_{Betz} as given by eq. (10), which was derived for the usual propeller type of windmill, is nearly always regarded as the maximum possible power output that can be obtained by any type of windmill. However, this is an incorrect interpretation of the expression. Betz's result was obtained by an analysis based upon actuator disc theory. The assumptions in his theory are, that the presence of the windmill causes a steady, axial force, acting on the air in a direction opposite to the undisturbed stream velocity U (fig. 4a).

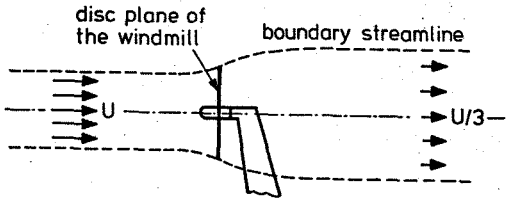

Fig. 4a. Conventional windmill.

If we consider types of windmills for which these assumptions are not valid, Betz's formula is not applicable. The research described in this paper found its origin in the question whether a type of windmill could be conceived having a power output per unit of frontal area larger than indicated by eq. (10).

The next step was the realization that physically, it is quite easy to imagine such a windmill. Let us assume a type of turbine where, in some as yet unspecified way, apart from the usual axial forces also forces are exerted on the air in a radial, outward direction (fig. 4b). The air would be deflected radially outwards, so that the radial forces would cause a diffuser effect. In consequence, the continuity of the flow requires the streamtube enveloping the windmill to have a larger diameter in front of the disc plane than it would have in the case of the usual windmill (fig. 4). The windmill generating radial forces would thus be able to absorb kinetic energy from a larger mass of air and could in principle have a larger power output for a given diameter.

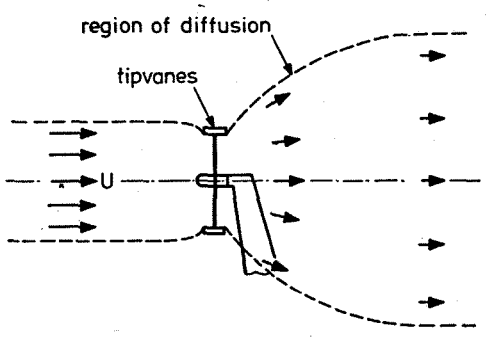

Fig. 4b. Windmill exerting radial forces.

In the language of theoretical aerodynamics, the physical process outlined above would be described as follows. If there is an aerodynamic force acting radially inwards on any windmill component (i.e. if that component applies a radial outward force to the air) this is associated with circulation. Symmetrically distributed radial forces in the disc plane would correspond to a distribution of vortex rings lying in the disc plane. This vorticity would, unlike the vorticity associated with the axial forces, remain confined to an area in the immediate vicinity of the disc plane itself. It would cause a net circulation in such a sense that a Venturi-type of flow is established, with the windmill disc in the narrowest part of the streamtube.

From this rather general discussion, it is seen that a ducted rotor is just one particular example of the application of the above described principle. An aerodynamic "lift" acts radially inwards on the ductsections, so that by reaction the air is deflected outwards, thus causing a diffuser effect. Put in another way again, the duct sections impose a Kutta condition such that the air flows off with the desired radial velocity component.

4. Description of tipvanes ("rotor winglets").

The configuration whose characteristics are discussed here is shown schematically in fig. 5 and is called the "tipvane system". The socalled tipvanes are small auxiliary wings mounted at the tips of the windmill blades. The wings are oriented such that their leading edge is approximately perpendicular to the relative local flow velocity, whereas their angle of attack with respect to the relative velocity causes a lift in the direction of the rotor centre. As the windmill itself causes a radial velocity in the vicinity of the blade tips, a certain amount of tilting as shown in fig. 5 is also needed. The tilt would be reversed in the case of a thrust producing rotor.

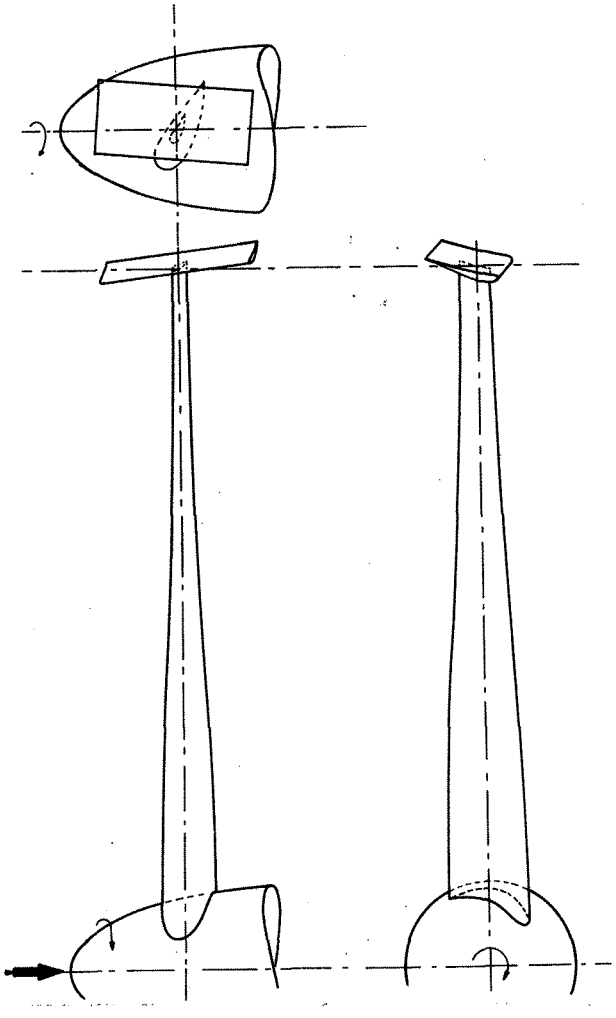

Fig. 5. Sketch of tipvane system.

In physical terms the functioning of the tipvane system is very easily explained: the rotating vanes deflect the oncoming airstream radially outwards, and thereby cause a diffuser effect. In terms of theoretical aerodynamics, however, some further explanation may be warranted. Let us consider linearized theory, where the trailing vortex sheets emanating from the tipvanes lie on a straight cylindrical surface with radius R and are carried away in axial direction with the undisturbed velocity V_o. Now let us also assume for a moment that the lift on the tipvanes is constant along the span, so that the trailing vorticity is concentrated in two discrete tipvortices. These tipvortices will trace out helical paths on the cylindrical surface (fig. 6).

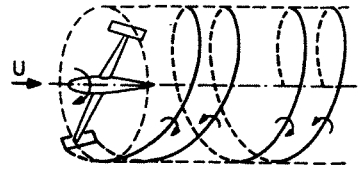

Fig. 6. Trailing vortices from tipvanes.

The flow associated with this vortex configuration is unsteady in an inertial frame of reference, e.g. a frame fixed to the supporting structure of the windmill. The time averaged flow field is obtained by taking the limit of an infinite number of tipvanes, taking care that the same radial force per unit length along the windmill circumference is generated by the infinite array of tipvanes as by the finite number of tipvanes. The helical vortices in this limit form a continuous, semi-infinite vortex-cylinder. Now it should be remembered that the tipvorticity emanating from the upstream vane-tips has equal strength but opposite direction compared with the vorticity coming from the downstream vane-tips. The two vortex cylinders associated with the upstream and downstream vane-tips cancel each other, except for a band of vorticity with a width equal to the span of the tipvanes (fig. 7). It is thus seen that again an overall circulation is established, similar to that of a duct, such that a Venturi-type of flow results. A more careful analysis given in ref. 1. shows that the same is true for the case of general spanwise liftdistributions along the tipvanes. Whether this linearized analytical model is indeed able to predict the time-average of the real flow was checked by experiments which will be described later in section 7.

5. Comparison between tipvanes and ducts.

It will be clear that the tipvanes need much less surface area than a full duct in order to generate a given radial force per unit length measured along the milldisc circumference. For a full duct the radial force f_{duct} per unit length is:

$$f_{duct} = C_{\ell_{duct}} \tfrac{1}{2} \rho w^2 c_{duct} \qquad (11)$$

where $C_{\ell_{duct}}$ = sectional lift coefficient of the duct,
w = axial velocity at the duct,
c_{duct} = duct chord

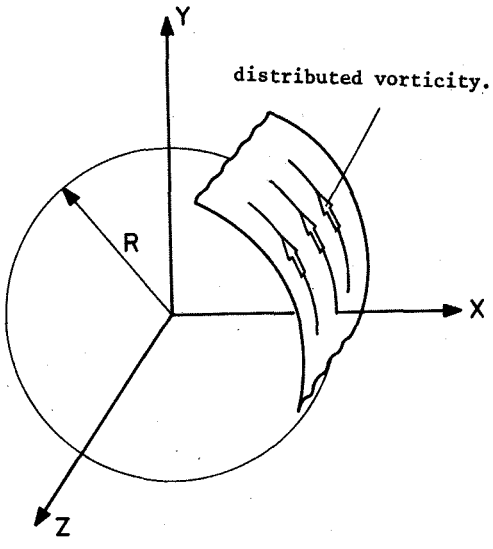

Fig. 7. Time-averaged analytical model of tipvane flow.

An order of magnitude estimate is obtained by substituting the windvelocity V_o for w into (11). In the case of the tipvane arrangement f_{vanes} is approximately given by

$$f_{vanes} = N.C_{L_{vane}} \tfrac{1}{2} \rho (\Omega R)^2 S_{vane} \cdot \frac{1}{2\pi R} \qquad (12)$$

where $C_{L_{vane}}$ = lift coefficient of the tipvanes
ΩR = tipspeed
N = number of vanes
S_{vane} = projected area per tipvane

Both $C_{\ell_{duct}}$ and $C_{L_{vane}}$ are limited by viscous effects to the same order of magnitude. In order to obtain a given value of the radial force, and thus to achieve a given mass flow augmentation, eqs. (11) and (12) show that the required areas of the tipvanes and the full duct have the ratio:

$$\frac{N.S_{vane}}{S_{duct}} \approx \left(\frac{V_o}{\Omega R}\right)^2 \text{ for a given mass flow augmentation} \qquad (13)$$

6. Theory of the mass flow augmentation by tipvanes.

As discussed in section 4, the linearized analytical model associated with the time-averaged flow field of the tipvanes consists of a band of vorticity along the circumference of the windmill disc (fig. 7). The average velocity increment in the disc plane due to this vorticity will be denoted by δV, and may be expressed like:

$$\delta V = \alpha \frac{\Gamma}{R} \qquad (14)$$

where Γ stands for the total circulation of the mentioned circumferential band of vorticity. The proportionality constant α is a function of the spanwise lift distribution along the tipvanes and is, according to an analysis given in ref. 1 and 2:

$$\alpha = \frac{1}{\pi} \{\ell n(\frac{R}{b/4}) + \tfrac{1}{4}\} \text{ (elliptical span loading)} \qquad (15)$$

where b is the span of the tipvanes.

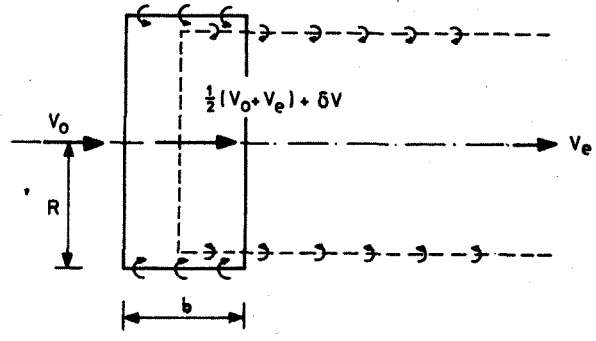

Fig. 8. Time-averaged analytical model of tipvane-turbine combination.

The axial forces associated with the basic windmill are represented in the linearized analytical model by a semi-infinite cylinder of vorticity (fig. 8). The velocity within the vortex-cylinder far downstream of the windmill is denoted by V_e. The velocity increment induced by the semi-infinite cylinder far downstream is thus $-(V_o-V_e)$. In the disc plane of the windmill the axial velocity increment due to the axial forces is half this value, namely $-\frac{1}{2}(V_o-V_e)$ and exactly at the "entrance-lip" of the vortex cylinder the increment is $-\frac{1}{4}(V_o-V_e)$. The average axial velocity in the disc plane of the windmill is thus given by $\frac{1}{2}(V_o+V_e)+\delta V$.

The velocity increment δV may be related to the radial forces as follows. The band of vorticity associated with the radial forces induces in its own plane a mean axial velocity of magnitude $\beta\,\Gamma/R$, with the proportionality constant β depending on the load distribution along the vane span (refs. 1 and 2):

$$\beta = \frac{1}{4\pi}\{\ell n(\frac{R}{b/32}) - \frac{5}{6}\} \text{ (elliptical span loading)} \qquad (16)$$

The total axial velocity in the plane of the vortex ring associated with the radial forces is thus:

$$w = V_o - \tfrac{1}{4}(V_o - V_e) + \beta \frac{\Gamma}{R} \qquad (17)$$

It may be shown (ref. 1) that Kutta-Youkowski's theorem may be applied, just as if the band of vorticity were considered as bound vorticity, so that

$$f_{vanes} = \rho\, w\, \Gamma \qquad (18)$$

Combining eqs. (14), (17) and (18) yields the

following relation between $\delta V/V_o$ and the magnitude of the radial forces:

$$\frac{f_{vanes}}{\rho V_o^2 R} = \frac{1}{\alpha}\left\{\frac{3}{4} + \frac{1}{4}\frac{V_e}{V_o} + \frac{\beta}{\alpha}\frac{\delta V}{V_o}\right\}\frac{\delta V}{V_o} \qquad (19)$$

For the value of V_e/V_o which yields optimum power the relation (19) is shown in fig. 9 (b/R = 0.5), in terms of power augmentation as a function of tipvane lift.

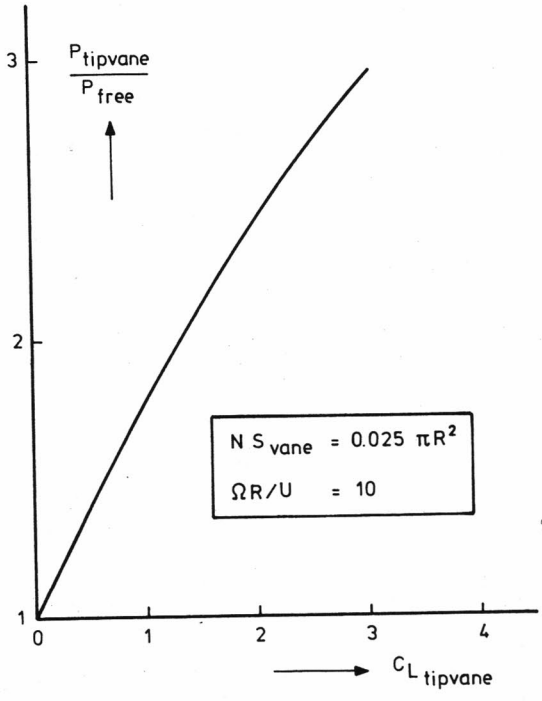

Fig. 9. Ideal power ratio of tipvane- and free turbine (no profile drag losses).

7. Experimental verification of the theory.

The windtunnel models used for the investigations that are presently described, were typical research-models: no attempt was done to study a complete turbine-tipvane combination. On the contrary, it was tried to isolate the aerodynamic effects due to the tipvanes alone.
A requirement for the model was that the total lift forces on the model tipvanes should have a value corresponding in a non-dimensional sense to full scale values. To achieve this at the low Reynolds-numbers tests, it was decided to choose larger values of the chord-diameter ratio than would be expected for full scale tipvanes. The tipvanes were mounted on rods having a circular cross section. The model diameter was approximately 0.70 m. The models were driven by a small electric motor at such a tipspeed that Reynolds numbers varied around a value of 150.000. A photograph of one of the models used is presented in fig. 10.

The sequence of photos shown in the figs. 11 and 12, taken from ref. 3, gives an explanation of the diffusor effect caused by the tipvanes.

Fig. 11 shows the flow when the model has just been started up; the rotational speed is still very low. One can see clearly the separate downwash regions induced by the passing of the tipvanes through the smoke jet. These regions of radial flow are bounded on both sides by tipvortices, the core of which is clearly visible in the photo.

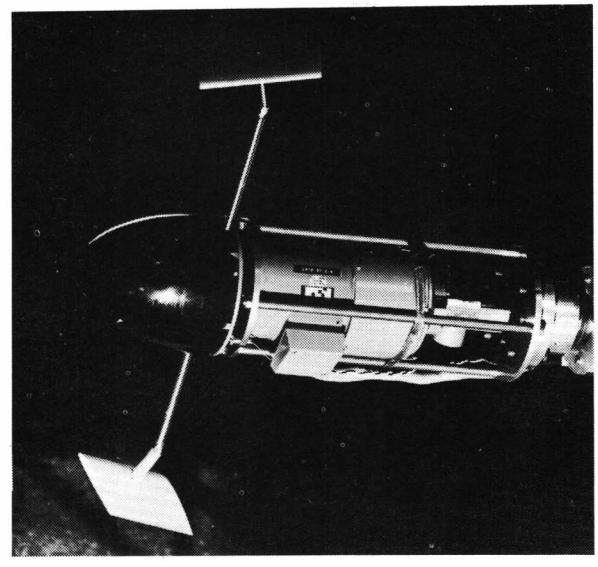

Fig. 10. Windtunnel model tipvanes.

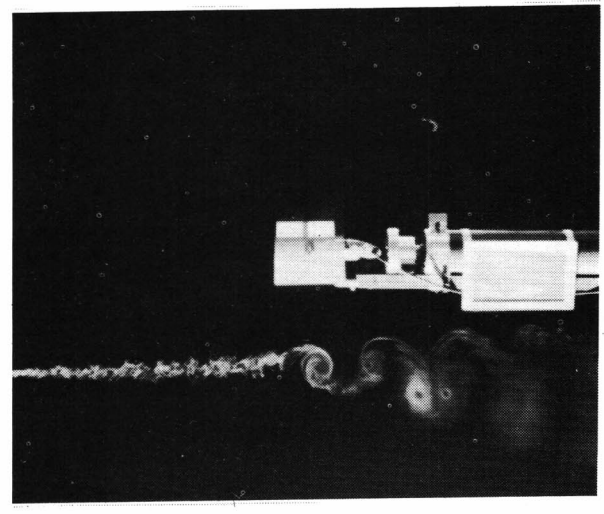

Fig. 11. Flow at small tipspeed.

At higher tipspeeds the tip vortices move closer to each other. There is a stronger tendency for the vortices to diffuse by mutual interaction. The final flow configuration has been reached in fig. 12, showing the situation for a tipspeed

ratio of approximately 10. The tipvortices have now vanished altogether by "swallowing" each other. In consequence, the separate radial flow regions have merged and a diffusor flow pattern has been established with a very large diffusor angle. The mentioned diffusion of the flow is associated with a general type of flow resembling a Venturi tube, although the tube is in the present case an immaterial one. The contraction of the flow in front of the rotor plane is shown clearly in fig. 12, as well as the large acceleration of the air near the rotor plane.

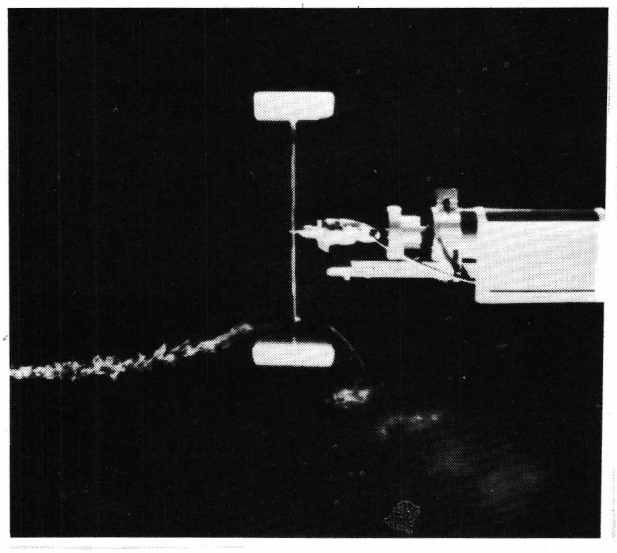

Fig. 12. Flow at $\Omega R/U \approx 10$.

The smoke pattern is asymmetric with respect to the rotor plane. In other words, the radius of a streamline is smaller in front of the windmill than at large distances downstream. This phenomenon implies, on account of the continuity equation, that the final velocity far downstream is smaller than the undisturbed velocity upstream. The cause is the drag component on the tipvane extension rods in longitudinal direction, (which component is proportional to the axial flow velocity and to the tipspeed), and a suction force on the ends of the tipvanes. From the photos taken it was concluded that the amount of drag in axial direction is of the same order as the drag generated by the normal type of turbine blades. In other words, in this respect a power turbine was simulated. Another working condition is shown in fig.13, i.e. an angle of attack of 13^{o}, an angle of tilt forward of 17^{o} (the tipvane "leans" opposite to the windspeed), and a tipspeed ratio of approximately 10. Some other streamlines are shown in fig. 14. The mass flow augmentation which is shown in the latter figure is of the order of 4 or 5 when compared with the normal turbine situation. This may be concluded by measuring the contraction of the flow in front of the turbine disc. Furthermore it should be realized that in the normal turbine situation there is no contraction, but on the contrary a divergence of the stream tube. The measured augmentation is in agreement with theoretical predictions.

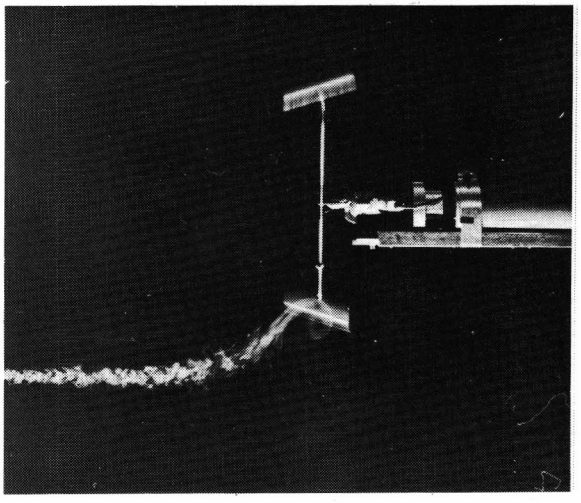

Fig. 13. Large contraction of streamtube.

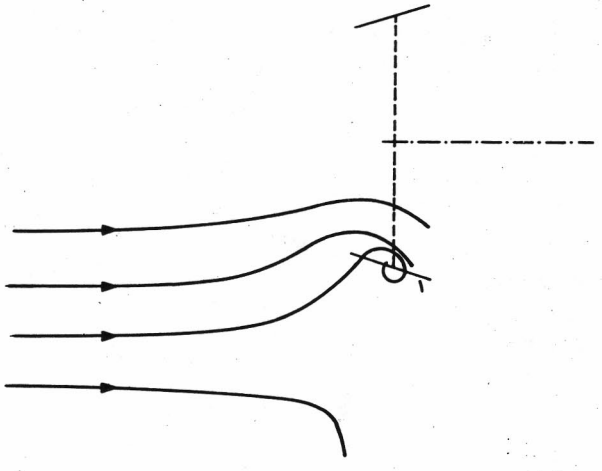

Fig. 14. Several streamlines at large diffusion ratio.

8. Tipvane induced drag.

The tipvanes are subject to two types of drag: the induced drag and the viscous drag.
The situation here will be comparable with a formation of migrating birds or airplanes. It is known that a V-formation is favourable to limit the induced drag, as a consequence of the mutual influence of the birds, who are flying partially in the area of upwash outside the wingtips of their predecessors.

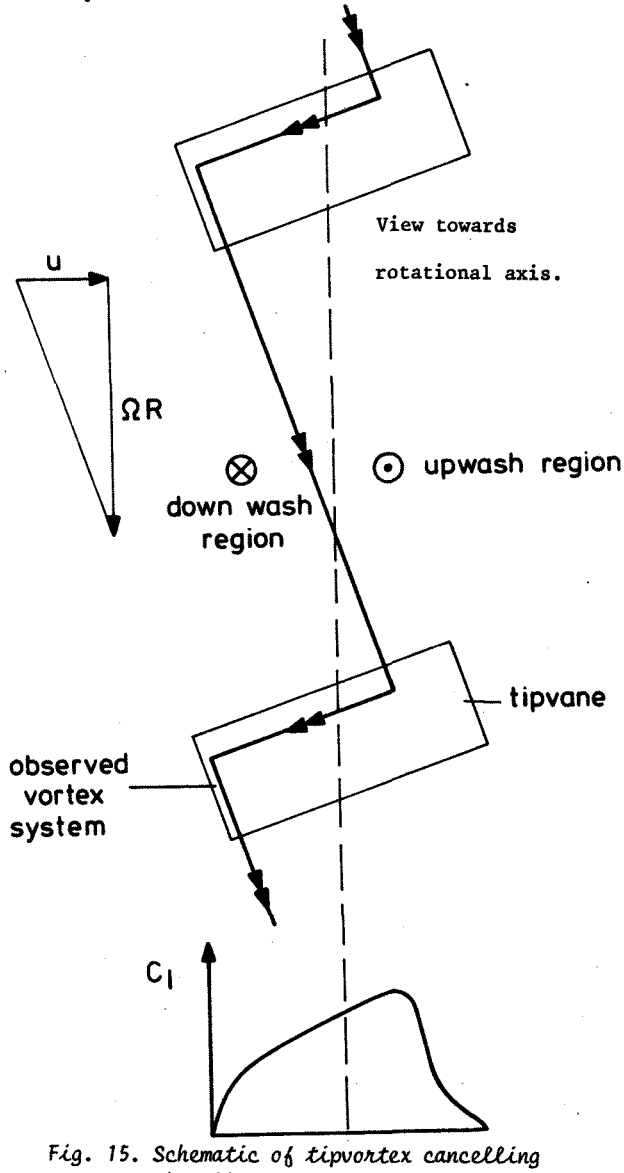

Fig. 15. Schematic of tipvortex cancelling process.

A theory for tipvanes (ref 1), based on the bird formation model, has shown that there are in principle two different possibilities to minimize the induced drag. The first possibility is to choose the span of rectangular vanes in such a way that a strong interaction of the tipvortices will exist (the vortices have to "swallow" each other).
The second possibility is to spread out the tipvortices as much as possible, by choosing a Concorde-like planform and properly twisting the vanes. In this case the trajectories of the tipvanes have to overlap partially each other relative to the air, so that a minimum of vorticity can be obtained in the wake.
In the mean time experiments have shown that in any case the first method can be realized in practice.
The flow situation where the vortex from the upstream tip of one vane exactly neutralises the downstream tipvortex of the next vane is called the synchronous state. It appears from the experiments that the tipvane system tends to automatically realize the synchronous state: the downstream part of the vane works in the outwash region of the preceding vane, and consequently carries little or negative lift (fig. 15). This means that from the point where a tipvortex hits the vane, automatically a counterrotating vortex is released, which causes the vortex cancelling.
A film will be shown as an illustration of the paper to show this process of vortex interaction. In the film it may be seen clearly that as a result a sort of saw tooth vortex is established around the turbine disc. Fig. 15 also shows a calculated lift distribution along the vane which gives rise to the effects already explained. One can see in this figure that at a certain point along the span, which coincides with the edge of the vortex sheet from the preceding vane, the lift drops sharply to a very low level.
A further substantiation of the process is shown in fig. 16, which shows a flow visualization of the boundary layer on the tipvane by using China Clay. Exactly at the point where according to the previous figure the lift drops, one can see a marked change in boundary layer development.

9. Observed boundary layer anomalies on rotating vanes.

After having studied in a very qualitative way the flow phenomena, some measurements were done of the drag level of the tipvanes. The first results obtained during these measurements indicated an unacceptably high drag level. This came as a bit of a surprise, because after having observed the vortex cancelling process described in the preceding chapter, there were no high values of induced drag expected. Furthermore care was taken during the design of the windtunnel model to use aerofoils which would work satisfactorily at the low Reynolds numbers used ($Re \tilde{=} 150.000$). This situation gave rise to the suspicion that perhaps the aerofoils did not behave as was expected from two-dimensional tests. It should be added that the aerofoil mean line in the rotating model was corrected for the curved path which is described by the tipvanes. For this reason some boundary layer studies were done.
The development of the boundary layer on the profile appeared to be entirely different than was found on stationary two-dimensional wing-sections. At angles of attack where the boundary layer on the lower surface of the tipvane aerofoils would normally be fully laminar, on the rotating model large separation bubbles occur. These bubbles grow in extent as the liftcoefficient increases, i.e. when the surface in question becomes more exposed to the main airstream! It is presently thought that centrifugal effects are responsible for these phenomena. Only the boundary layer air, being dragged along with the tipvane, is subject to centrifugal effects. All the other

air passes without appreciable rotation through the turbine disc, when looking in an inertial frame of reference.

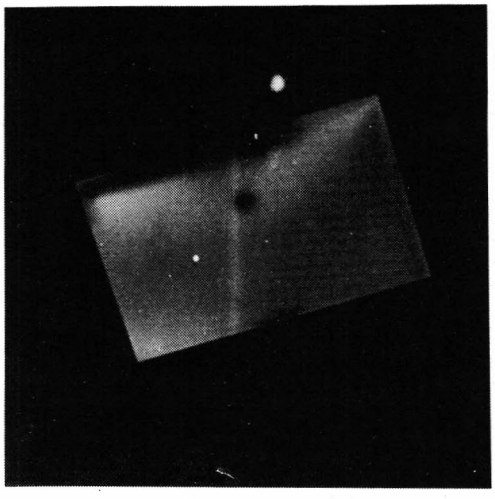

Fig. 16. Flow of fig. 15 visible in boundary layer (China Clay visualization on rotating tipvane, outer surface).

A substantial effort will have to be put into the development of special aerofoil sections for the tipvanes. A start has been made (ref. 4) to investigate carefully the nature of the centrifugal effects to which the boundary layer is subjected. This knowledge will then have to be taken into account during the design of aerofoils that, for the tipvane application, already have to meet rather unusual requirements. One of the requirements is, that a positive (nose-up) zero-lift pitching moment is needed, because this is favourable to reduce the parasitic power losses. A contradictory requirements is, that $C_{\ell_{max}}$ should be as high as possible, because this will help to reduce the tipvane area. All this must be achieved without appreciable flow separation, in order to keep the frictional drag as low as possible.

10. Conclusions

Tipvanes can induce a large mass flow augmentation through rotors, and are in this respect very well comparable with ducts. The amount of augmentation can be estimated roughly by a relatively simple theory, which has been confirmed by experiments. Whether tipvanes are interesting in actual application will largely depend on the power lost to overcome their drag, in comparison with the power saved by the mass-induction effects.
The induced drag of tipvanes is small. The cause of this was determined both by theoretical and experimental investigations. It appears that, just as in the case of ducts, almost no vorticity is left in the flow. On the other hand, the optimization of the profile drag of tipvanes is complicated by boundary layer anomalies, found during experiments and presently ascribed to rotational effects.

If it is assumed that by further research the lift/drag performance of the tipvane sections can be improved to a level such as achieved by usual aerofoilsections, then the application of tipvanes to rotors might be very interesting.
An example may illustrate this.

A prediction by the above indicated theory which was separately confirmed by experiments (ref. 1) is, that the ratio between the total radial force and the axial force needed for eliminating the slipstream contraction of a hovering rotor is:

$$\frac{T}{f_{vanes} \cdot 2\pi R} = \sqrt{3} \quad \text{(no slipstream contraction)}$$

The powergain ΔP due to the elimination of the slipstream contraction is:

$$\Delta P = T\, v_{i_{free}} \quad (1 - 1/\sqrt{2})$$

where $v_{i_{free}}$ denotes the induced velocity in the rotorplane of a free rotor delivering the same thrust. The powerloss due to tipvane drag can in this particular case be expressed as:

$$\frac{P_{loss}}{\Delta P} = \frac{C_D}{C_L} \frac{\Omega R}{v_{i_{free}}} \frac{1}{(1 - 1/\sqrt{2})\sqrt{3}} \quad \text{(no slipstream contraction).}$$

which amounts to a relatively small ratio, if the tipvanes are properly shaped so that their lift/drag ratio is sufficiently high. The last formula also indicates that application of tipvanes becomes more favourable as the rotorloading becomes higher.

11. References.

1. Th. van Holten: "Performance analysis of a windmill with increased power output due to tipvane induced diffusion of the airstream", Delft University of Technology, Dept. of Aerospace Engineering, Memorandum M-224, November 1974.

2. Th. van Holten: "Higher-order asymptotic expressions for the velocity field of a propeller duct or an array of tipvanes in axisymmetric flow", Delft University of Technology, Dept. of Aerospace Eng., Memorandum M-280, June, 1977.

3. G.J.W. van Bussel, Th. van Holten, G.A.M. van Kuik: "Flow visualization study of the functioning of tipvanes", Delft University of Techn., Dept. of Aerospace Eng., Memorandum M-295, February 1978.

4. G.J.W. van Bussel, Th. van Holten, G.A.M. van Kuik: "Flow visualization study of the boundary layer on rotating tipvanes", Delft University of Technology, Dept. of Aerospace Eng., Memorandum M-302, March 1978.